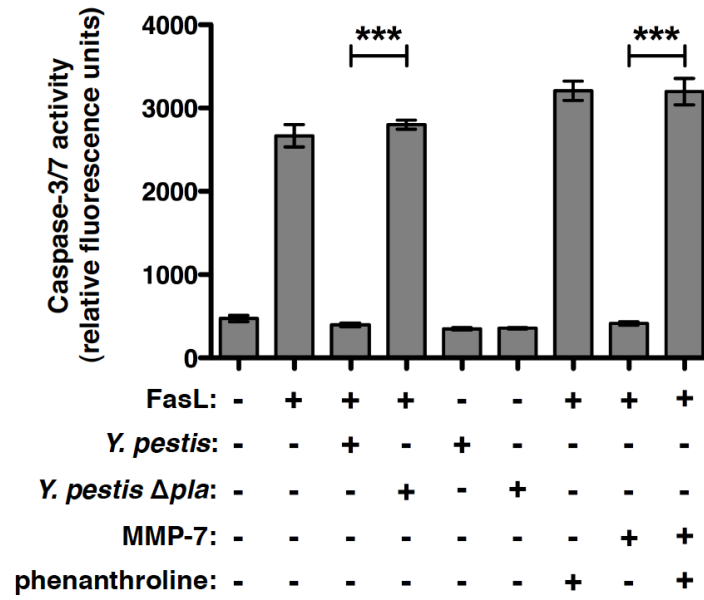


**Figure S1. Degradation of FasL requires catalytically active Pla, related to Figure 1. (A)**

Pla immunoblot of *E. coli* induced to express *pla* or carrying empty vector, *Y. pestis* strains, and purified Pla. The lower *Y. pestis* band represents a cross-reactive non-specific protein and numbers to the left indicate molecular weight in kDa. (B) Plasminogen activation by *E. coli*, *Y. pestis*, and purified Pla. (C) Immunoblot analysis of plasminogen (Plg), tumor necrosis factor alpha (TNF $\alpha$ ), and glycoprotein Ib alpha chain (GPIIb- $\alpha$ ) incubated with *Y. pestis*, *Y. pestis*  $\Delta$ *pla*, or *Y. pestis* producing the D206A *pla* active site point mutant. (D) Immunoblot analysis of recombinant human and mouse FasL incubated with *Y. pestis*, *Y. pestis*  $\Delta$ *pla*, or *Y. pestis* D206A *pla*.



**Figure S2. Pla inhibits FasL-induced caspase-3/7 activation in A549 cells, related to**

**Figure 2.** FasL was pretreated with *Y. pestis* or MMP-7 for processing before addition to A549 cells, a human type II pneumocyte cell line. Caspase-3/7 activation was measured based on binding of the fluorescent substrate Ac-DEVD-AMC. FasL processing by either protease inhibits caspase-3/7 activation in A549 cells. Phenanthroline was used as an MMP-7 inhibitor.  $n = 3$  for all groups and this experiment was repeated 3 times. \*\*\* $P < 0.001$ .



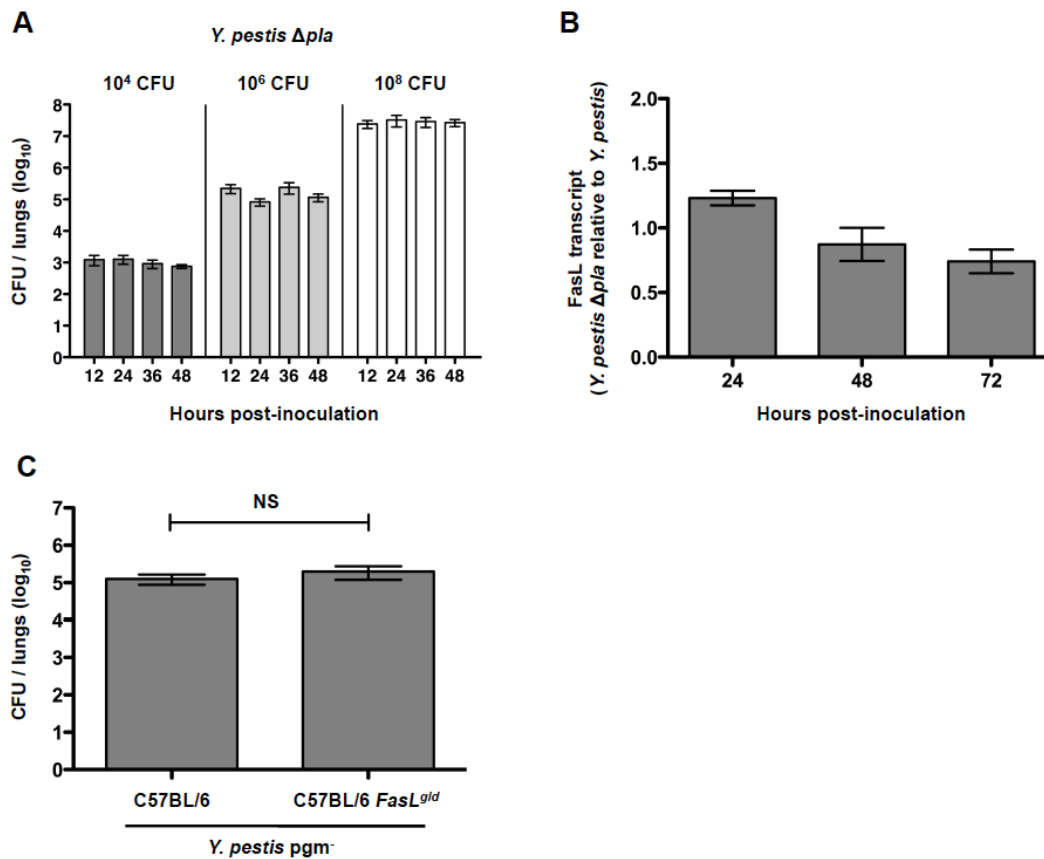


**Figure S3. Bacterial CFU in the lungs using various inoculum concentrations, *FasL* transcript levels in the lungs, and bacterial burden of the attenuated strain *Y. pestis*  $pgm^-$ , related to Figure 3.** (A) C57BL/6 mice were inoculated via the intranasal route with increasing doses of *Y. pestis*  $\Delta pla$  –  $10^4$ ,  $10^6$ , or  $10^8$  CFU. At the times indicated, mice were sacrificed and lung homogenates plated to enumerate CFU. For a given inoculum, CFUs are maintained in the lungs between 12 and 48 h. Recovered CFUs are approximately one log lower than input inoculum.  $n = 5$  for all groups and this experiment was repeated twice. (B) *FasL* mRNA transcript levels from lungs of mice infected with *Y. pestis*  $\Delta pla$  as fold change relative to those infected with *Y. pestis* for each corresponding time point. Total lung RNA was extracted from 3 mice per time point for each of *Y. pestis* and *Y. pestis*  $\Delta pla$  infections. (C) CFU at 48 h in the lungs of mice infected i.n. with  $10^7$  CFU of the attenuated strain *Y. pestis*  $pgm^-$ .  $n = 10$  for each group representing data combined from two independent experiments. NS = not significant.

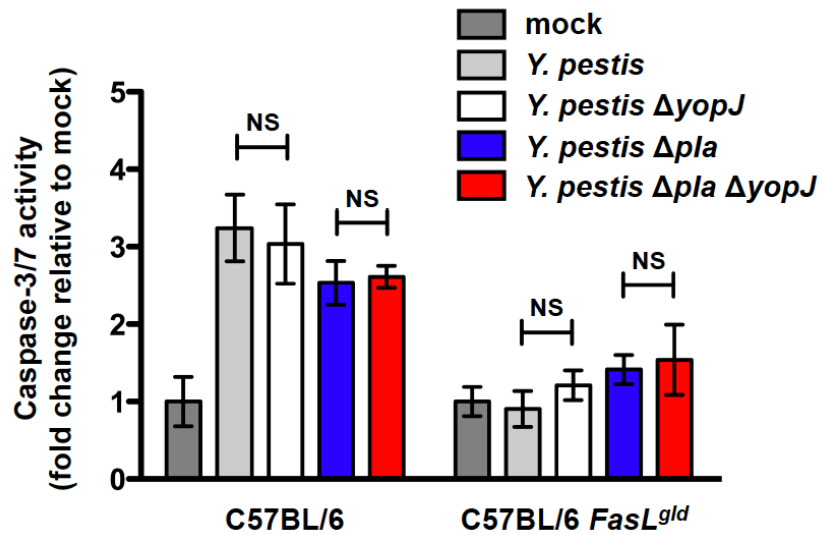


**Figure S4. The contribution of YopJ to caspase-3/7 activation in the lungs, related to Figure 4.** YopJ does not contribute to caspase-3/7 induction in the lungs during the pro-inflammatory phase of pneumonic plague either in the presence or absence of Pla. Caspase-3/7 activity was measured after 48 h from perfused lung homogenates of C57BL/6 or C57BL/6 *FasL<sup>gld</sup>* mice infected i.n. with *Y. pestis* or the  $\Delta pla$ ,  $\Delta yopJ$ , or  $\Delta pla \Delta yopJ$  double mutant strains. Caspase-3/7 activity is represented as fold change relative to mock infection values.  $n = 5$  for all groups and this experiment was repeated twice. NS = not significant.

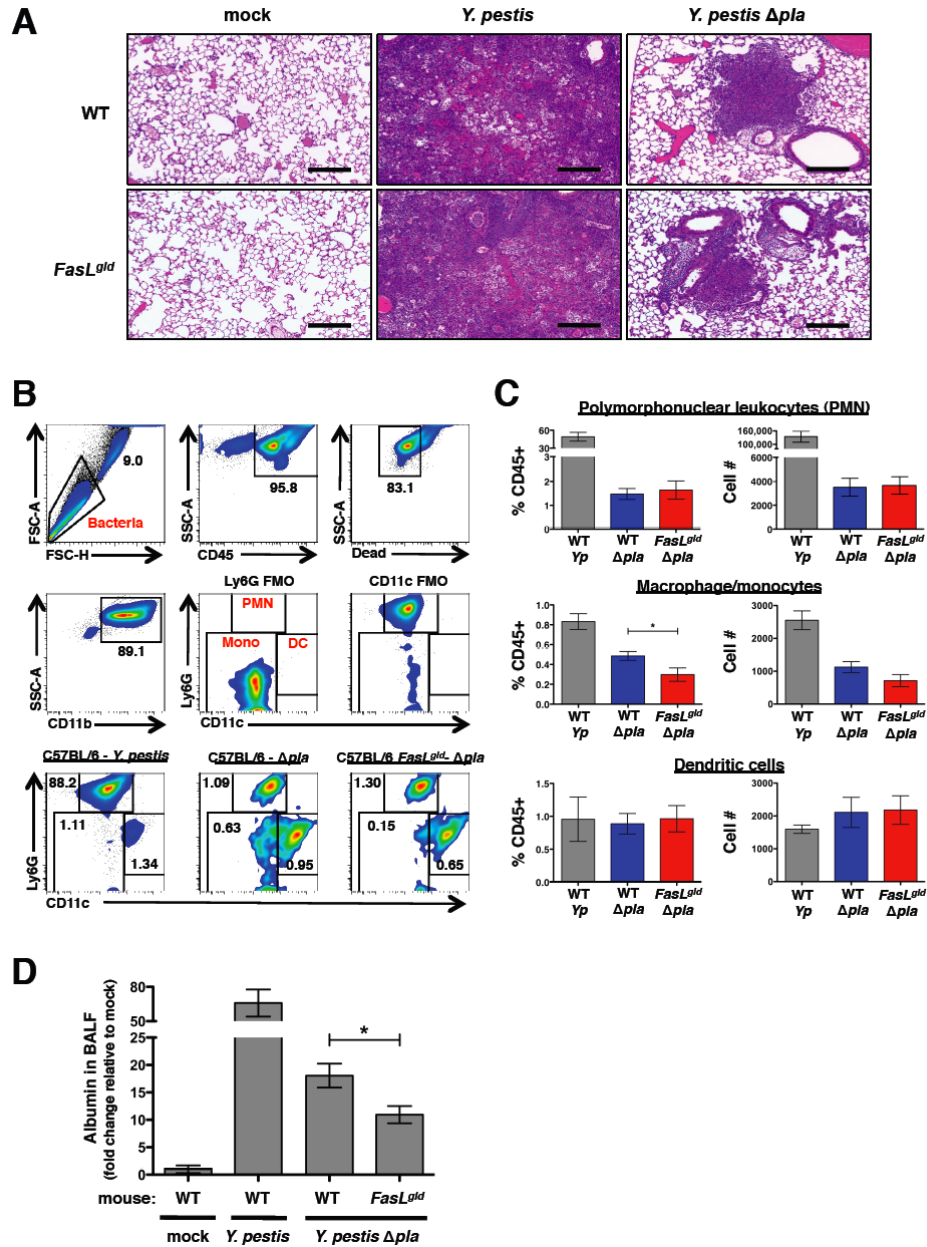


**Figure S5. Hematoxylin and eosin (H&E) staining of mouse lung tissue, immune cell quantification, and lung injury during pneumonic plague, related to Figure 5. (A) At 48 h post-inoculation with PBS (mock), *Y. pestis*, or *Y. pestis*  $\Delta pla$ , C57BL/6 or C57BL/6 *FasL<sup>gld</sup>* mice were sacrificed, the lungs inflated and fixed with 10% formalin, and processed for histological staining with H&E. Representative images of inflammatory lesions are shown. The size and abundance of inflammatory lesions comprised of primarily polymorphonuclear leukocytes**

(PMNs) are enhanced in mice infected with fully virulent *Y. pestis*; little difference is observed between wild-type and *FasL<sup>gld</sup>* mice infected with the equivalent strain. Scale bars represent 2 mm. (B) Immune cell quantification from bronchoalveolar lavage fluid. Example gating scheme and fluorescence minus one (FMO) negative controls. Bacterial cells were excluded through negative gating after comparison to bacteria only controls. The remaining cells were positively gated based on viability, CD45, CD11b, CD11c, and Ly6G expression. PMNs were identified as the CD45<sup>+</sup> CD11b<sup>+</sup> CD11c<sup>-</sup> Ly6G<sup>+</sup> population, macrophage/monocytes as the CD45<sup>+</sup> CD11b<sup>+</sup> CD11c<sup>-</sup> Ly6G<sup>-</sup> population, and dendritic cells as the CD45<sup>+</sup> CD11b<sup>+</sup> CD11c<sup>+</sup> Ly6G<sup>-</sup> population. (C) Immune cell populations were quantified by total cell numbers and by percentage of total CD45<sup>+</sup> cells. *n* = (6 for WT *Yp*; 8 for WT  $\Delta$ *pla*; 10 for *FasL<sup>gld</sup> Δpla*) and this experiment was repeated twice. (D) Albumin quantification from bronchoalveolar lavage fluid. Mice were inoculated via the intranasal route with *Y. pestis* or *Y. pestis*  $\Delta$ *pla* and bronchoalveolar lavage fluid (BALF) was collected after 48 h. To assess alveolar permeability, mouse albumin was quantified by ELISA and graphed as fold change relative to mock-infected animals. *n* = (3 for WT mock; 6 for WT *Yp*; 8 for WT  $\Delta$ *pla*; 10 for *FasL<sup>gld</sup> Δpla*) and this experiment was repeated twice. \*P < 0.05.

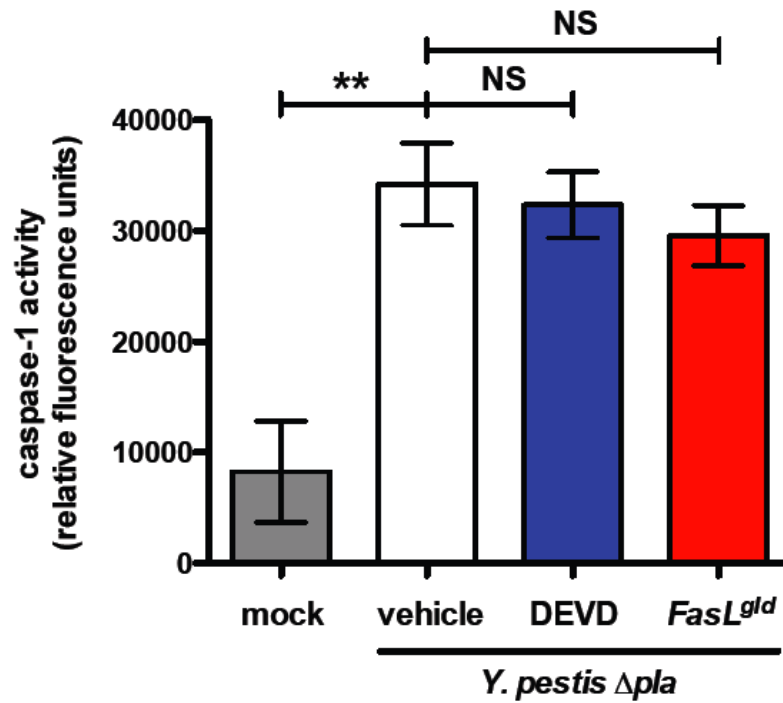


**Figure S6. DEVD does not affect caspase-1 activity *in vivo*, related to Figure 6.** Mice were infected with *Y. pestis*  $\Delta$ *pla* and treated with either DEVD or vehicle alone. DEVD was administered at 0 and 24 h post-inoculation via the i.p. route. As a specificity control for DEVD treatment, caspase-1 activity was determined from whole lung homogenates at 48 h post-inoculation using the FLICA caspase-1 detection kit (ImmunoChemistry Technologies).  $n = 3$  for all groups and this experiment was repeated twice. \* $P < 0.05$  and NS = not significant.